

AD-A137 257

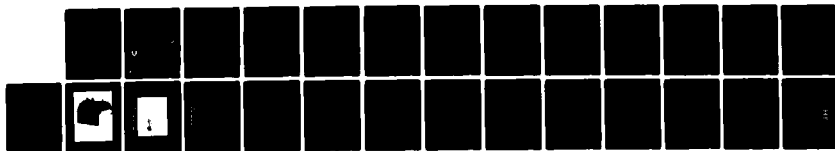
DYNAMIC COMPACTION OF CERAMIC MATERIALS(U) ARMY
ARMAMENT RESEARCH AND DEVELOPMENT CENTER ABERDEEN
PROVING GROUND MD BALLISTIC RESEARCH LAB
G L MOSS ET AL. DEC 83 ARBRL-MR-03327

1/1

UNCLASSIFIED

F/G 19/1

NL



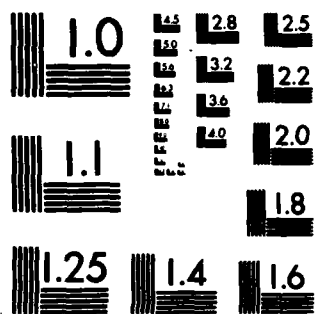
END

DATE

FILED

2 84

DTIC



MICROCOPY RESOLUTION TEST CHART
NATIONAL BUREAU OF STANDARDS-1963-A

AD A 137257

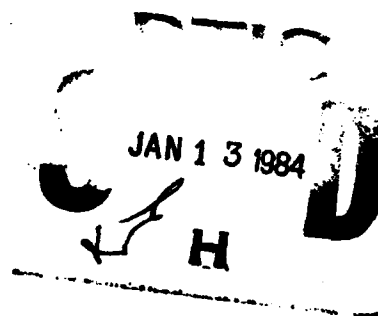
(12)

ADF 300 370

MEMORANDUM REPORT ARBRL-MR-03327

DYNAMIC COMPACTION OF CERAMIC MATERIALS

Gerald L. Moss
Ralph F. Benck
Paul H. Netherwood, Jr.
John R. Stratton



December 1983



US ARMY ARMAMENT RESEARCH AND DEVELOPMENT CENTER
BALLISTIC RESEARCH LABORATORY
ABERDEEN PROVING GROUND, MARYLAND

Approved for public release; distribution unlimited.

DTIC FILE COPY

84 01 13 131

Destroy this report when it is no longer needed.
Do not return it to the originator.

Additional copies of this report may be obtained
from the National Technical Information Service,
U. S. Department of Commerce, Springfield, Virginia
22161.

The findings in this report are not to be construed as
an official Department of the Army position, unless
so designated by other authorized documents.

*The use of trade names or manufacturers' names in this report
does not constitute endorsement of any commercial product.*

UNCLASSIFIED

SECURITY CLASSIFICATION OF THIS PAGE (When Data Entered)

REPORT DOCUMENTATION PAGE		READ INSTRUCTIONS BEFORE COMPLETING FORM
1. REPORT NUMBER MEMORANDUM REPORT ARBRL-MR-03327	2. GOVT ACCESSION NO. AD-A137 257	3. RECIPIENT'S CATALOG NUMBER
4. TITLE (and Subtitle) DYNAMIC COMPACTION OF CERAMIC MATERIALS		5. TYPE OF REPORT & PERIOD COVERED Memorandum Report Oct 81 - Sep 82
		6. PERFORMING ORG. REPORT NUMBER
7. AUTHOR(s) Gerald L. Moss, Ralph F. Benck, Paul H. Netherwood, Jr., John R. Stratton		8. CONTRACT OR GRANT NUMBER(s)
9. PERFORMING ORGANIZATION NAME AND ADDRESS US Army Ballistic Research Laboratory, ARDC ATTN: DRSMC-BLT(A) Aberdeen Proving Ground, MD 21005		10. PROGRAM ELEMENT, PROJECT, TASK AREA & WORK UNIT NUMBERS Proj. Element 6.11.01A DA Proj. No. 1L161101A91A AMCMS Code 61110191A
11. CONTROLLING OFFICE NAME AND ADDRESS US Army AMCCOM, ARDC Ballistic Research Laboratory, ATTN: DRSMC-BLA-S(A) Aberdeen Proving Ground, MD 21005		12. REPORT DATE December 1983
14. MONITORING AGENCY NAME & ADDRESS (if different from Controlling Office)		13. NUMBER OF PAGES 25
		15. SECURITY CLASS. (of this report) Unclassified
16. DISTRIBUTION STATEMENT (of this Report) Approved for public release; distribution unlimited.		15a. DECLASSIFICATION/DOWNGRADING SCHEDULE
17. DISTRIBUTION STATEMENT (of the abstract entered in Block 20, if different from Report)		Accession For NTIS GRA&I <input checked="" type="checkbox"/> DTIC TAB <input type="checkbox"/> Unannounced <input type="checkbox"/> Justification By Distribution/ Availability Codes Dist Avail and/or Special A'
18. SUPPLEMENTARY NOTES		
19. KEY WORDS (Continue on reverse side if necessary and identify by block number) Explosives, Powder Compaction, Powder Consolidation, Detonation Velocity		
20. ABSTRACT (Continue on reverse side if necessary and identify by block number) Progress relative to the explosive compaction of hot metallic and ceramic materials is described. The compaction technique, explosive characterization and initial computations of compaction with a two-dimensional Lagrangian finite-difference computer code TROTT are described. Computed results are shown to indicate how sample, container, explosive and unloading waves influence the compaction process.		bet X6050

TABLE OF CONTENTS

	<u>Page</u>
LIST OF ILLUSTRATIONS.	5
I. INTRODUCTION	7
II. PROCEDURE.	7
III. RESULTS.	10
IV. CONCLUSIONS.	11
REFERENCES	21
DISTRIBUTION LIST.	23

LIST OF ILLUSTRATIONS

<u>FIG. NO.</u>		<u>Page</u>
1	Schematic of experimental technique used to determine explosive detonation rates.	13
2	Barrier to protect equipment from explosive blast	14
3	Gage resistance versus time for the determination of the detonation rate of amatol (1.27 cm thick, 0.94 g/cm ³)	15
4	A comparison of detonation rate measurements for amatol and DETASHEET	16
5	Computed compaction of a plate of porous copper (1.90 cm thick, 2.6 g/cm ³) between plates of amatol (3.99 cm thick) detonated at the left. The porous copper was bounded on both sides by plates of solid copper (0.635 cm thick), and this was separated from the explosive with an insulator (HASH 60, 0.635 cm thick).	17
6	Computed compaction of porous aluminum to illustrate the effect of a container on the stress histories and compaction of the powder.	
	Vertical lines indicate boundaries between materials. The Al powder is in the center in both figures. Fig. 6a shows the powder compressed directly between plates of PETN. Explosive products were not allowed to penetrate the powder. Fig. 6b shows the compression when there is a Mo layer between the PETN and the powder.	
	The graphs show stress distributions at one time after the start of detonation (Fig. 6a -- 17.6 μ sec; Fig. 6b -- 18.3 μ sec). Initiation was along a plane at the bottom, and detonation sweeps from the bottom to the top.	
	Dotted horizontal lines indicate vertical locations where pressures (solid lines) are plotted as a function of horizontal distance through the explosively loaded systems. Each horizontal line locates zero on the vertical pressure scale for the vertical location it (dotted horizontal line) also identifies.	18
7	Computed compaction of porous Cu (29 percent of theoretical density) illustrating less than complete compaction. This is indicated by the low pressures (unresolvable in the figure) attained in the powdered Cu. The Cu is bounded on both sides with plates of solid Cu (0.635 cm thick), and these were loaded symmetrically with amatol (3.99 cm thick) explosions along the other sides of the solid Cu. The amatol was initiated from the bottom end of the system as shown above. The dotted and solid lines have the same meaning as described under Fig. 6.	19

LIST OF ILLUSTRATIONS (CONT'D)

FIG. NO.

Page

- | | | |
|---|--|----|
| 8 | <p>Computed compaction of porous Cu (60 percent of theoretical density). While only incomplete compaction was attained in the computation illustrated in Fig. 7, complete compaction is indicated above with the high pressures developed in the compressed powder. Even though only 2.0 cm of amatol was detonated on each side of the container - powder system in this case, total compaction was attained because the initial powder density was higher than for the computation illustrated in Fig. 7. The dotted and solid lines have the same meaning as described under Fig. 6</p> | 20 |
|---|--|----|

I. INTRODUCTION

There appear to be numerous worthwhile reasons to advance dynamic loading techniques for the processing and compaction of materials. For example, there is the potential for (1) reducing the cost of sintered and, especially, hot-pressed materials, (2) preparing void-free high-melting-point materials, (3) consolidating pure materials that must be alloyed for practical sintering, and (4) retaining special properties, phases, defects or degrees of crystallinity during powder compaction. Dynamic compaction can be accomplished by a variety of techniques, but the objectives of this program are to accomplish the following:

- A. Explosively compact hot metallic and ceramic powders.
- B. Explosively enhance the sinterability of ceramic powders.
- C. Investigate material properties only attainable with dynamic compaction.

In the following, progress will be described relative to the first objective. The second objective is being pursued for us by Prof. Palmour, and the third objective will be pursued as the explosively processed and compacted materials are obtained.

II. PROCEDURE

Dynamic loading with line initiated explosives is being used in an attempt to form planar compacts. In this configuration, the detonation wave propagates from one end of the sample to the other, and the problems are to attain uniformly compacted flat samples and, then, to recover them intact.

A wide range of loading conditions is possible with the different types of explosives available. Depending on the explosive, the detonation characteristics can be a function of the thickness, density and confinement used. Several explosives have been obtained for experimental versatility. These are listed in Table I along with the Chapman-Jouguet (CJ) pressures and detonation rates for select thicknesses and densities.

Explosive characterizations were requested from the manufacturers, but only limited information was obtained. Detonation velocities were furnished for the AMATOL (CIL), ammonium nitrate-sodium nitrate mixture (IRECO) and the ammonium nitrate-waxed PETN mixture (Trojan), although the Trojan SWP-9 mixture has not been received. The detonation velocities for the remaining explosives

in Table I were obtained from published reports.¹⁻⁵ Nothing about the detonation pressures was obtainable from the manufacturers, and our only alternative was to estimate them from the detonation velocities for our pretest considerations. These estimates were made with an equation that gives the CJ pressure P_{CJ} as

$$P_{CJ} = \frac{\rho_o D^2}{1 + \gamma}, \quad (1)$$

where γ is approximately 3, ρ_o is the initial explosive density and D is the detonation velocity. The pressures listed in Table I were determined with Eq. 1.

In general, there is an interest in attaining a steady detonation process to cause uniform compaction and, thereby, avoid subsequent cracking. However, local detonation irregularities can arise from inhomogeneities in an explosive, and the method of initiation can influence detonation over an appreciable region bounding the initiation site. We had little prior knowledge about these details so continuous detonation velocity and pressure measurements are being made to furnish information critical to the compaction process.

Pressures are to be recorded with Manganin piezoresistive gages, and detonation velocities are being measured with a wire-in-tube resistance gage described by Ribovich et al.⁶ A schematic of the measuring technique is shown in Fig. 1.

A special furnace with molybdenum disilicide heating elements has been ordered for working temperatures up to 1600°C. This is a high-cost item that must be protected from explosive blast during compaction. Either the furnace

¹B. M. Dobratz, "LLNL Explosives Handbook. Properties of Chemical Explosives and Explosive Simulants," Lawrence Livermore National Laboratory Report No. UCRL-52997, March 1981.

²L. Penn, F. Helm, M. Finger, and E. Lee, "Determination of Equation of State Parameters for Four Types of Explosives," Lawrence Livermore Laboratory Report No. UCRL-51892, August 1975.

³B. Crossland and J. A. Cave, Proceedings, 5th International Conference on High Energy Rate Fabrication, University of Denver Research Institute, Colorado, 1975, pp 4.9.0-4.9.11.

⁴M. A. Cook, E. B. Mayfield, and W. S. Partridge, "Reaction Rates of Ammonium Nitrate in Detonation," *J. Phys. Chem.*, **59**, 1955, pp 675-680.

⁵H. C. Hoenig, E. L. Lee, M. Finger, and J. E. Kurrle, "Equation of State of Detonation Products," Proceedings, 5th Symposium (International) on Detonation, Ed. S. J. Jacobs and R. Roberts, Superintendent of Documents, Washington, D.C., 1970, pp 503-512.

⁶J. Ribovich, R. W. Watson, and F. C. Gibson, "Instrumented Card-Gap Test," *AIAA J.*, **6**, 1968, pp 1260-1263.

or the explosion can be isolated, but there is some advantage in protectively containing the furnace and letting the explosive products expand freely. This is the approach being pursued, and a photograph of the protective barrier for the furnace is shown in Fig. 2. This barrier is a 1.68 m (5.5 ft) outside diameter by 3.66 m (12 ft) long steel cylinder with 15.2 cm (6 in) thick walls. The plan is to heat the powders within this cylinder and, then, move them with a remotely operated transfer device to a compaction site far enough from the cylinder to avoid damage to the furnace, but near enough for the compaction to be completed while the powder is still hot.

Computations of the compaction are underway to supplement the experimental work and assist with the interpretation of results. These are being conducted with the two-dimensional Lagrangian finite-difference computer code TROTT.⁷ The pressure in the solid P_s is assumed to be given by the Mie-Grüneisen equation of state

$$P_s = C\mu + D\mu^2 + S\mu^3 + \Gamma\rho(E - E_H), \quad (2)$$

where ρ is the density, $\mu = \rho/\rho_0 - 1$, ρ_0 is the initial density, E is the internal energy at density ρ , E_H is the internal energy along the Hugoniot and Γ is the Grüneisen ratio. C , D and S are the constant coefficients of the Hugoniot.

Plastic deformation of solids is based on the Reuss incremental plasticity relations, and the effective plastic strain $\Delta\bar{\epsilon}^P$ is given by

$$\Delta\bar{\epsilon}^P = (\bar{\sigma}^N - \bar{\sigma})/3G, \quad (3)$$

where $\bar{\sigma}$ is the effective stress equated to the yield criterion Y , G is the shear modulus and $\bar{\sigma}^N$ is a term with the same form as the effective stress $\bar{\sigma}$, but formed from the nominal stress $\sigma'_{ij}{}^N$ that would occur if the strain were entirely elastic. The elastic strain follows from the deviator stress σ'_{ij} given by

$$\sigma'_{ij} = \sigma'_{ij}{}^N \cdot \frac{Y}{\bar{\sigma}^N}, \quad (4)$$

and the elastic stress-strain relation.

Compaction is treated by fitting the consolidation curve with a series of four parabolic segments.⁸ Within each segment, the curve is defined by the pressures at each end of the segment and by an increment ΔP which is the

⁷L. Seaman and D. R. Curran, "TROTT Computer Program for Two-Dimensional Stress Wave Propagation," Ballistic Research Laboratory Contract Report No. ARBRL-CR-00428, April 1980 (Unclassified) (AD A085788).

⁸Lynn Seaman, Robert E. Tokheim, and Donald R. Curran, "Computational Representation of Constitutive Relations for Porous Materials," Defense Nuclear Agency Contract Report No. DNA 3412F, May 1974 (Unclassified).

pressure difference between the straight line connecting the end points and the parabola measured midway between the specific volumes at the limits of the segment. Consolidation is specified by the critical pressure P_c at which this occurs, and the corresponding pressure is determined with the Mie-Grüneisen equation.

III. RESULTS

In preliminary tests of the detonation-velocity gage, high-frequency noise was superimposed on the records of the gradual voltage decay corresponding to the propagation of the detonation wave along the length of the resistance wire. The cause of this noise is still unknown, but it would tend to mask other effects such as a slope change as the detonation proceeded from initiation to a steady state. To avoid the noise, signals are processed with a 100 kHz low-band-pass filter. A record obtained with the filter is shown in Fig. 3. The slope of this record changes intermittently throughout the entire recording interval, and there is no run-in time that is clearly distinguishable from these intermittent changes. Apparently, the detonation of the DETASHEET initiator was either insufficiently different from the AMATOL for this to be a distinguishable effect or the run-in time was too short to resolve. However, records of the detonation rate of AMATOL and DETASHEET are clearly different as shown in Fig. 4. This indicates the recording technique is sensitive to the characteristics of the particular explosive being tested.

There is, however, still some uncertainty about the detonation-velocity measurements. Repetitive tests and measurements have resulted in inconsistent results. The values recorded for AMATOL are 3.32, 2.71 and 3.69 mm/ μ sec for explosive thicknesses of 1.27, 2.00 and 2.54 cm, respectively. The reason for the low value of 2.71 mm/ μ sec is unknown, and further tests are under way to clarify the situation.

The computer computations have been particularly enlightening and give a clear impression of how the loading geometry, initial sample density and the pressure pulse affect compaction. An example is shown in Fig. 5 of a computation that illustrates the treatment of a two-dimensional flow of several materials and interfaces. The compaction is of copper powder (29 percent of theoretical density ρ_t) in a solid copper container insulated at the top and bottom with a layer of $Al_2O_3-SiO_2$ (HASH 60). The compression is symmetrical and between two plates of AMATOL that were initiated at the left along a vertical plane perpendicular to the figure. With this configuration the detonation waves move from left to right. A wedge type collision zone is a well known characteristic of this type of loading, and the cell distortion makes this evident in Fig. 5.

An indication of the influence of a powder container during compaction is shown in Fig. 6. In the compaction shown at the left, the explosive was in direct contact with the porous aluminum, but the explosive products were not allowed to penetrate the interface. In contrast, the computation shown at the right is for the same situation as at the left except the explosive and powder are separated by a layer of molybdenum. In both cases, the stresses at the cell boundary, which are identified with the horizontal lines, are plotted

vertically with zero stress located at the cell boundary. Without the container, noticeable stresses develop in the powder, but when there is a layer of molybdenum separating the explosive from the powder, only low stresses develop in the powder and they occur much further behind the detonation front than when there is no container. These results imply that the container can influence compaction substantially.

The initial density of the powder is similarly shown to be a governing factor during compaction. For example, no stresses are computed to develop in 29 percent dense copper loaded symmetrically between 4 cm plates of AMATOL as shown in Fig. 7. In contrast, intense stresses are computed to develop in 60 percent dense copper when compressed with only 2 cm of AMATOL (Fig. 8).

Densities are also computed throughout the course of compaction, and in keeping track of these, it was found that when intense stresses fail to develop in the powder, the compaction is incomplete. Presumably, stresses equal to the flow stress are attained since considerable consolidation occurs even though theoretical density is not achieved.

Finally, 60 percent dense copper powder was actually compacted symmetrically with 2 cm of AMATOL on each side. The recovered sample was considerably cracked, at least in part, by unloading waves, but a final density greater than 97 percent of theoretical density was attained. The computations suggested that theoretical density should have been attained, and since it essentially was, it is concluded that the computations can be effectively used to get an idea of what actually happens during dynamic compaction.

IV. CONCLUSIONS

Preliminary results suggest the following about the AMATOL, resistance-wire detonation-rate gage and the compaction process.

1. The measured detonation velocity of AMATOL, 2.54 cm thick and compressed to a density of 1.02 g/cm^3 , is $3.69 \text{ mm}/\mu\text{sec}$. This is in approximate agreement with the velocity of $3.65 \text{ mm}/\mu\text{sec}$ reported by the manufacturer.
2. Repetitive detonation velocity measurements with the resistance-wire gage have been erratic and indicate that refinements in the measuring technique, or an alternative method, may be desirable.
3. Computations indicate that powder density, explosive thickness, powder container and unloading waves have pronounced effects on the compaction process and the product formed.

TABLE I. PROPERTIES OF EXPLOSIVES

TYPE	COMPOSITION	SOURCE	DENSITY g/cc	THICKNESS OR DIAMETER cm	DETONATION VELOCITY mm/μsec	C-J PRESSURE* Gigapascals
AMATOL	80% Ammonium Nitrate 20% TNT	CIL	1.02	N/A	3.65	3.4
ANFO	94% Ammonium Nitrate 6% Fuel Oil	duPont	0.82	3.0 40.6	1.6 5.3	0.54 5.97
ANFO	88% Ammonium Nitrate 12% Fuel Oil	Laboratory Mixture	0.9	3.0 4.0 7.9 8.6	1.25 1.55 2.05 2.10	0.35 0.54 0.79 0.99
AN-TNT	50% Ammonium Nitrate 50% TNT	Laboratory Mixture	1.0	1.3 2.5 5.0 24.6	1.82 2.99 3.79 4.71	0.83 2.24 3.59 5.50
SWP-9	Ammonium Nitrate, Waxed PETN	Trojan	1.04	1.27 3.18	1.68 2.44	0.73 1.55
DBA-10HV	Ammonium Nitrate Sodium Nitrate	IRECO	1.25	1.25 2.54 3.79 7.62	2.33 3.40 3.89 4.20	1.65 3.61 4.73 5.51
PETN	PETN SuperFine	duPont	0.25 0.48 0.99 1.53 1.76	4.45 3.81 2.54 2.54 5.08	2.83 3.60 5.48 7.49 8.28	0.7** 2.4 8.7 22.5 33.8

$$*P_{CJ} = \frac{\rho_o D^2}{\gamma + 1}, \gamma \approx 3$$

**P_{CJ} values from Reference 5

EXPLOSIVE DETONATION RATES

GAGE RESISTANCE vs TIME

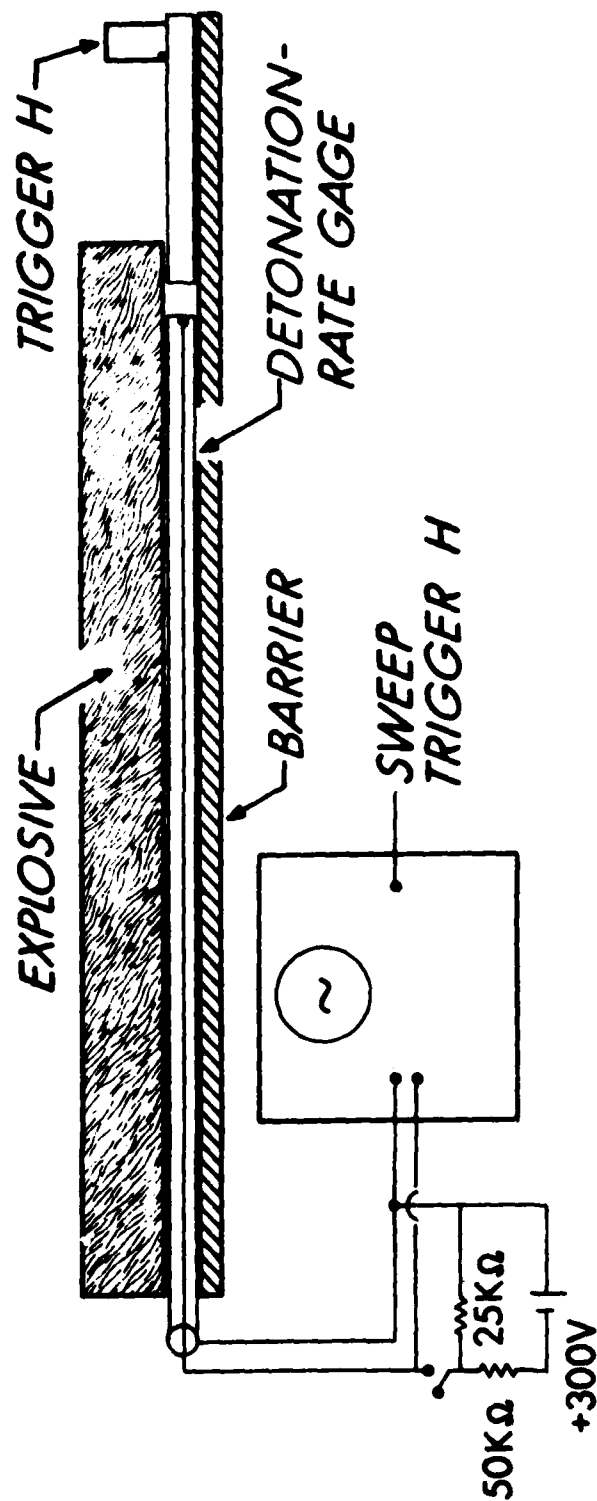


Figure 1. Schematic of experimental technique used to determine explosive detonation rates.

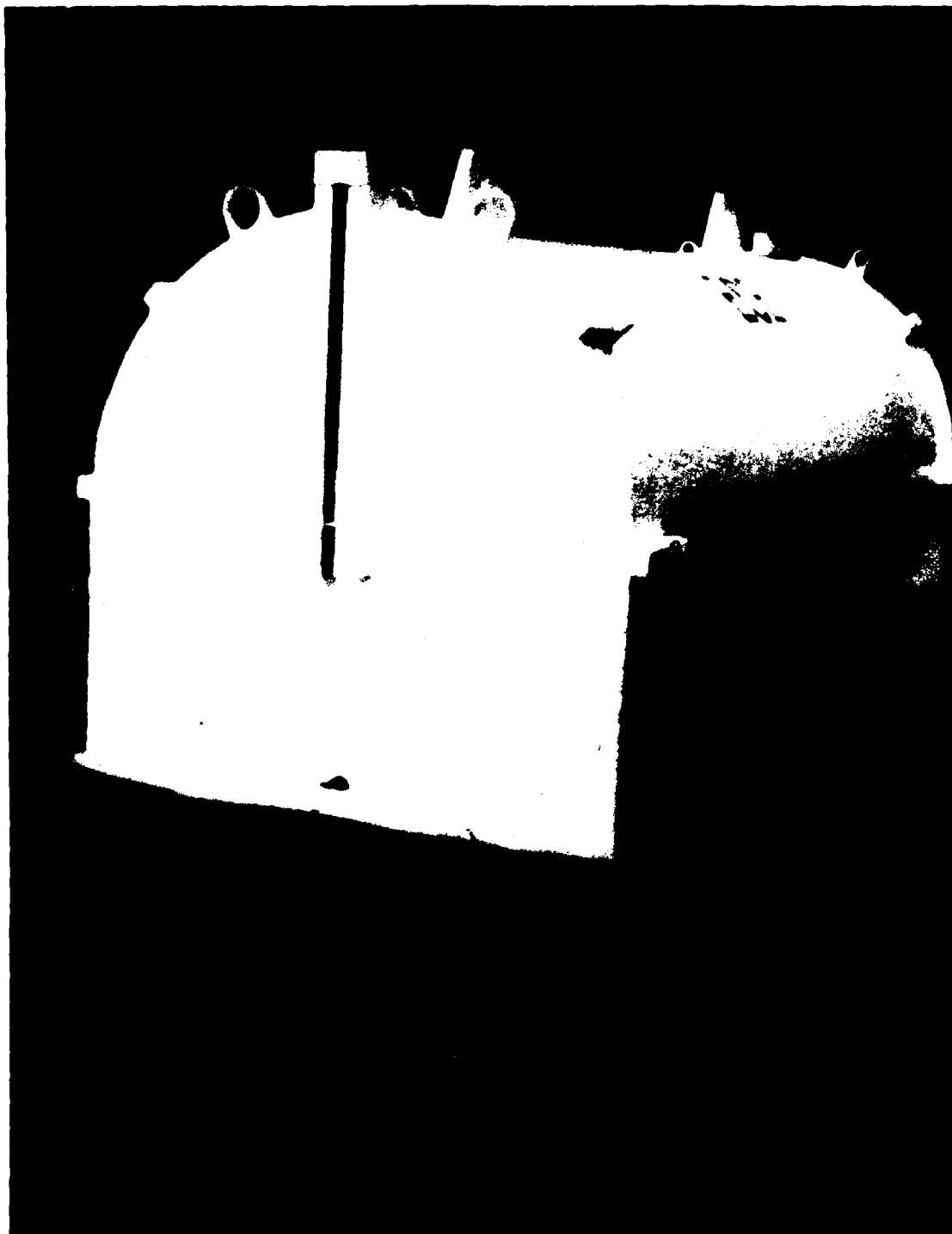


Figure 2. Barrier to protect equipment from explosive blast.

AMATOL DETONATION RATE

GAGE RESISTANCE vs TIME

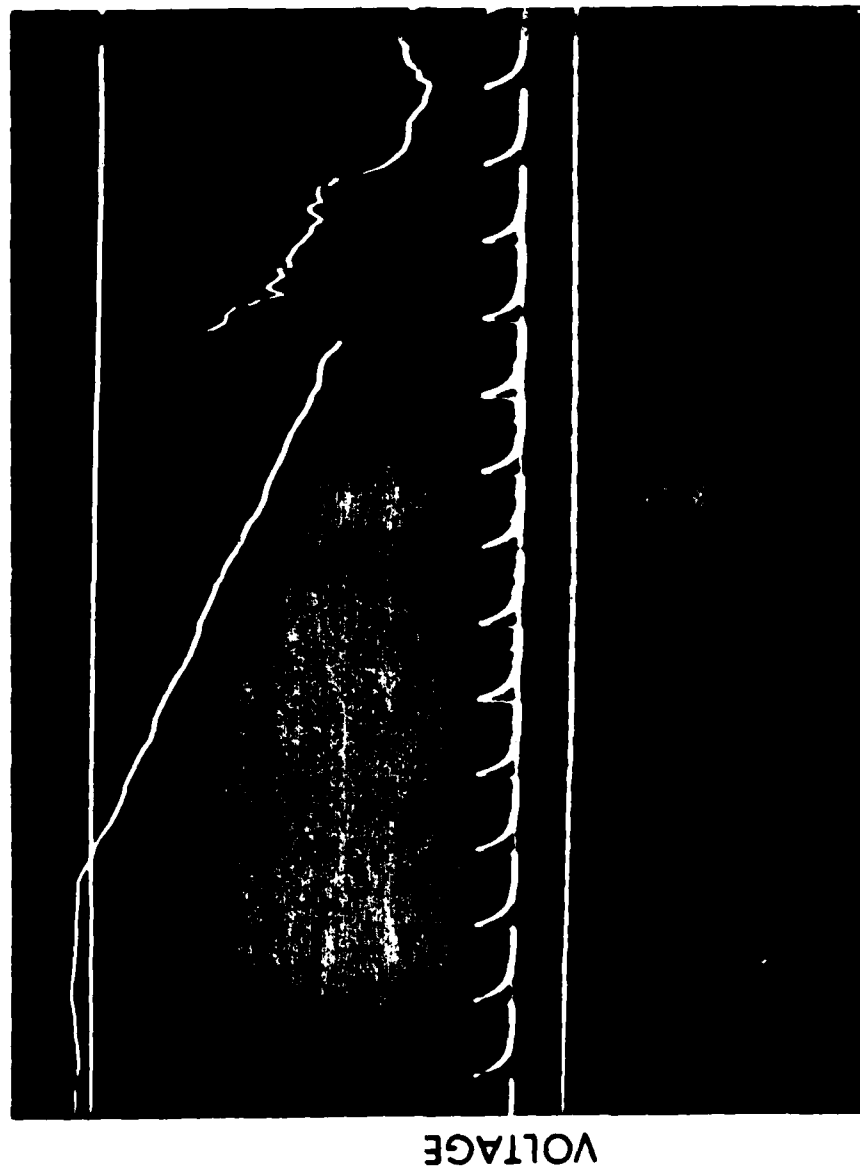


Figure 3. Gage resistance versus time for the determination of the detonation rate of amatol (1.27 cm thick, 0.94 g/cm³).

EXPLOSIVE DETONATION RATES

GAGE RESISTANCE VS TIME

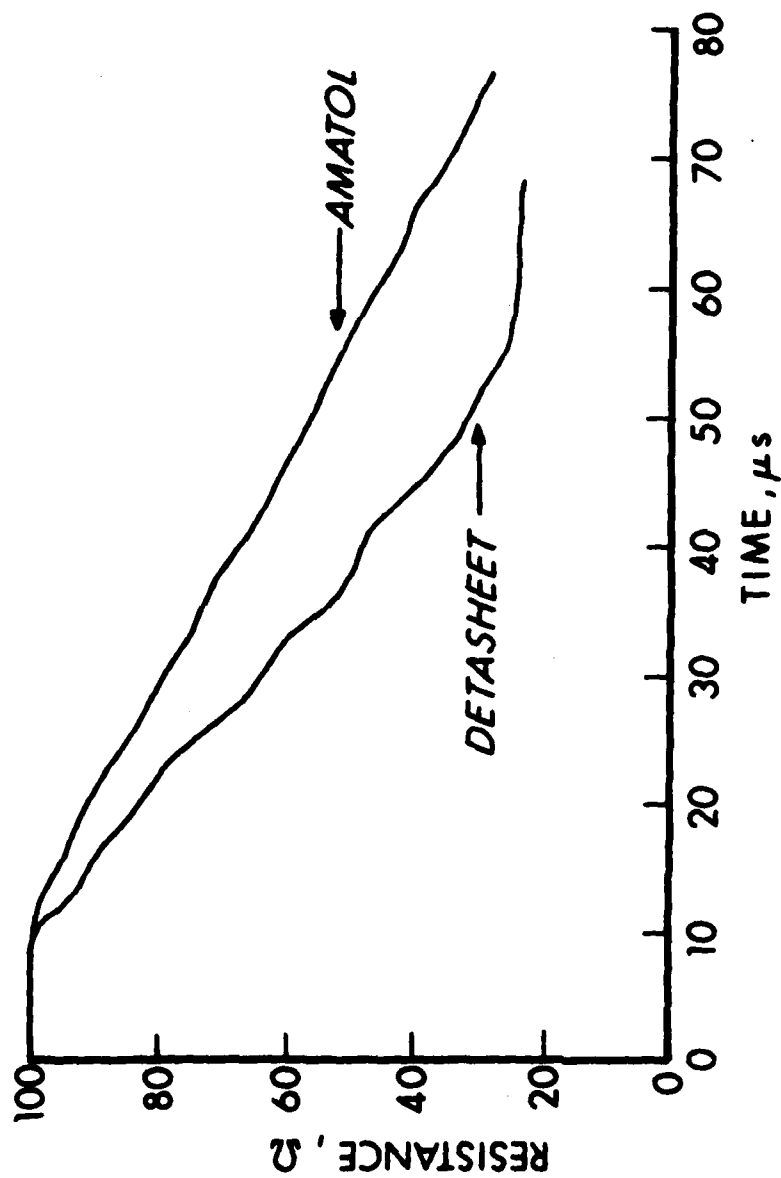


Figure 4. A comparison of detonation rate measurements for amatol and DETASHEET.

COMPUTED COMPACTION

AMATOL (1.57 in) - HASH 60 (1/4 in) - Cu (1/4 in) - POROUS Cu
Cu (3/4 in thick, 2.6 g/cm³)

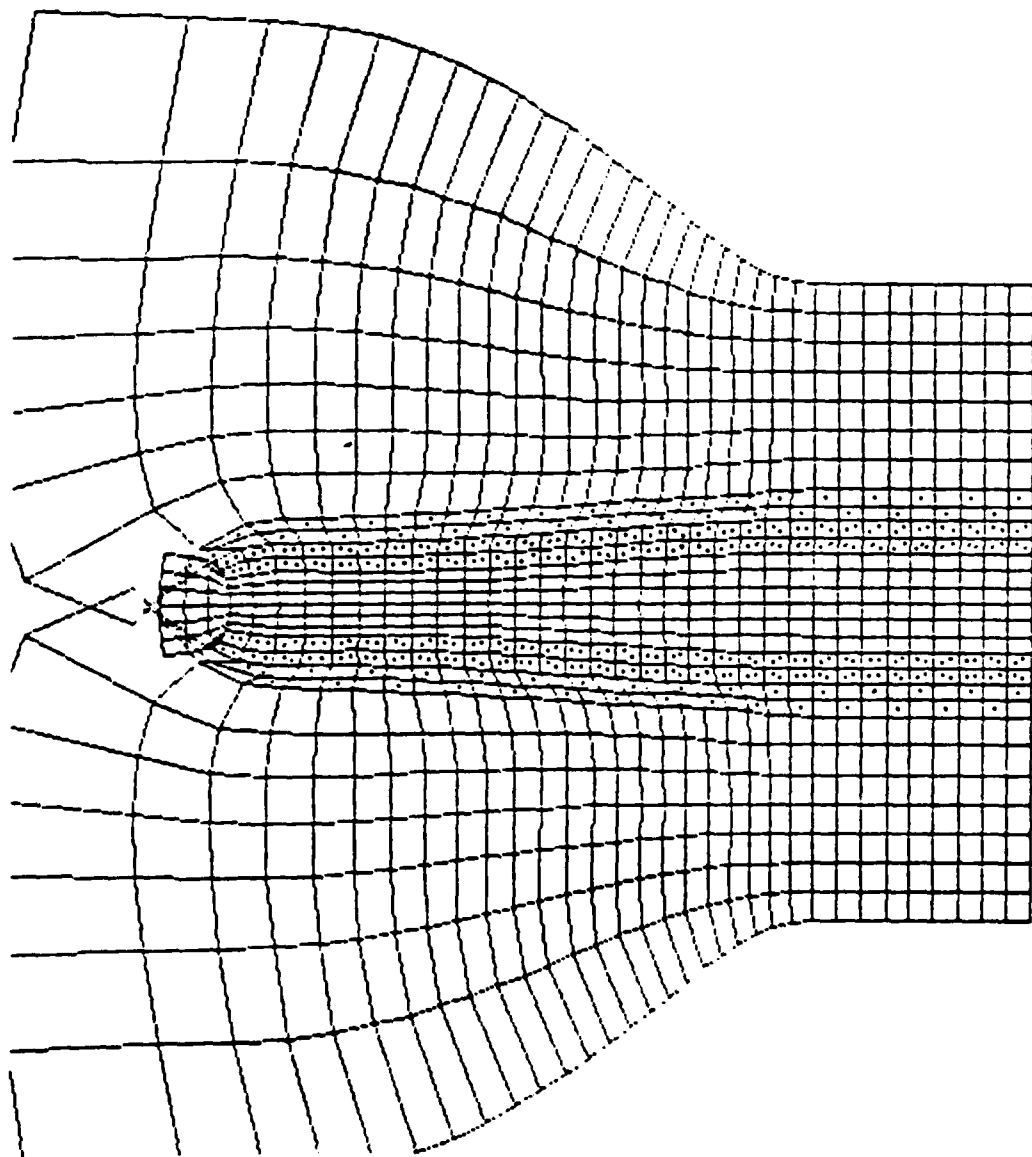


Figure 5. Computed compaction of a plate of porous copper (1.90 cm thick, 2.6 g/cm³) between plates of amatol (3.99 cm thick) detonated at the left. The porous copper was bounded on both sides by plates of solid copper (0.635 cm thick), and this was separated from the explosive with an insulator (HASH 60, 0.635 cm thick).

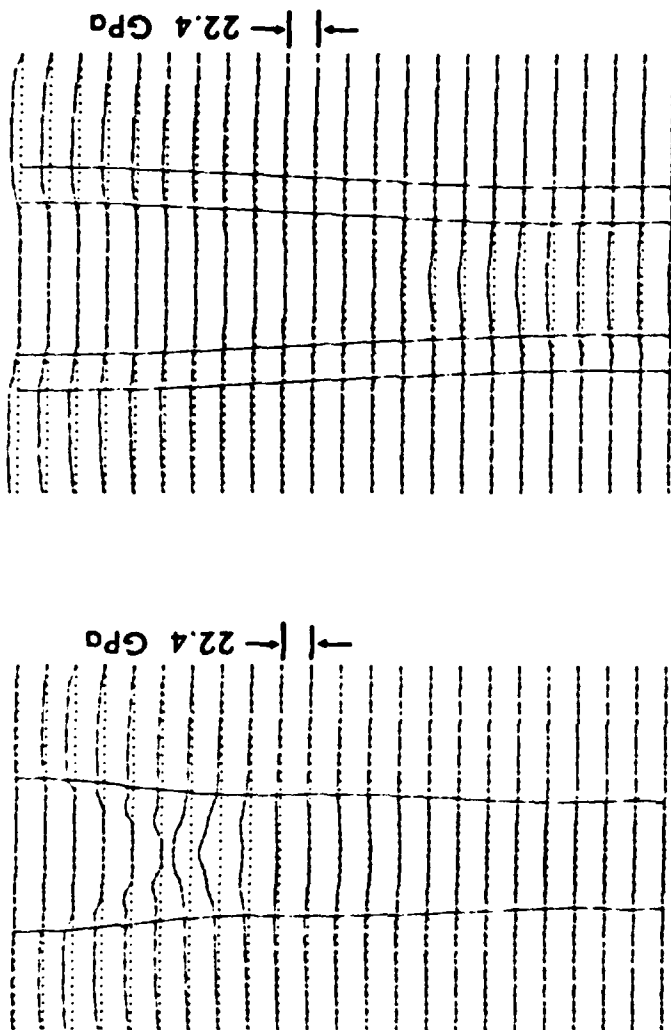


Figure 6. Computed compaction of porous aluminum to illustrate the effect of a container on the stress histories and compaction of the powder.

Vertical lines indicate boundaries between materials. The Al powder is in the center in both figures. Fig. 6a shows the powder compressed directly between plates of PETN. Explosive products were not allowed to penetrate the powder. Fig. 6b shows the compression when there is a Mo layer between the PETN and the powder.

The graphs show stress distributions at one time after the start of detonation (Fig. 6a -- 17.6 μ sec; Fig. 6b -- 18.3 μ sec). Initiation was along a plane at the bottom, and detonation sweeps from the bottom to the top.

Dotted horizontal lines indicate vertical locations where pressures (solid lines) are plotted as a function of horizontal distance through the explosively loaded systems. Each horizontal line locates zero on the vertical pressure scale for the vertical location it (dotted horizontal line) also identifies.

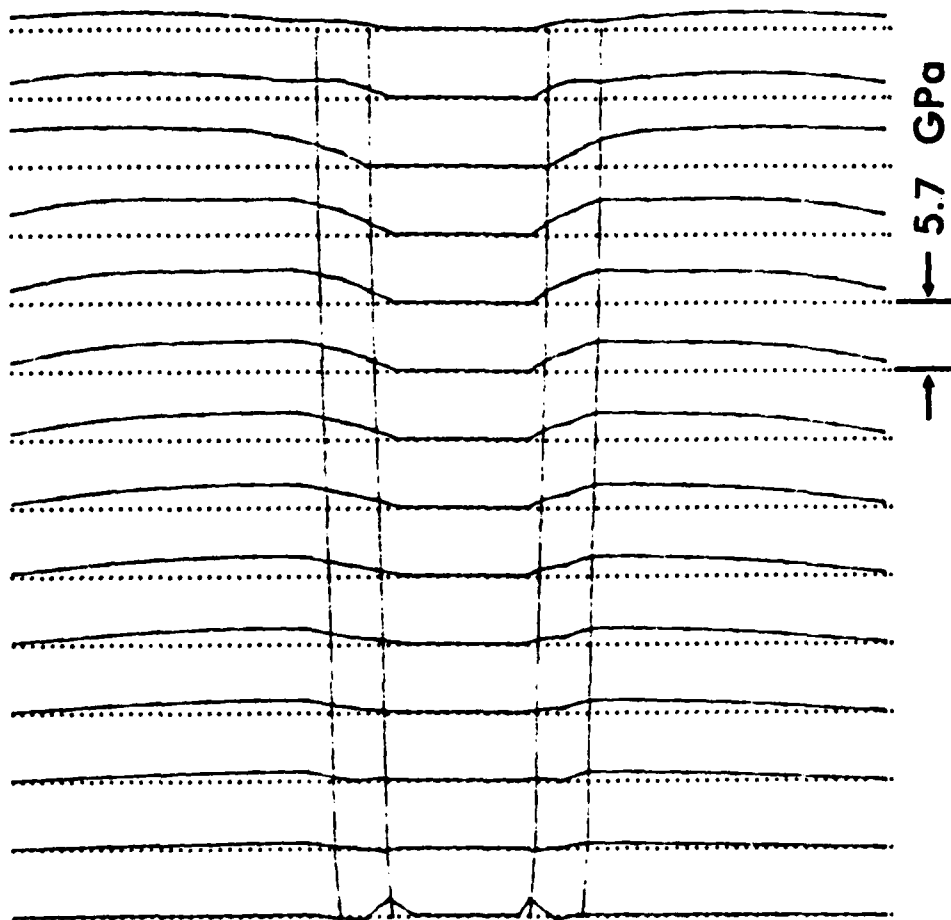


Figure 7. Computed compaction of porous Cu (29 percent of theoretical density) illustrating less than complete compaction. This is indicated by the low pressures (unresolvable in the figure) attained in the powdered Cu. The Cu is bounded on both sides with plates of solid Cu (0.635 cm thick), and these were loaded symmetrically with amatol (3.99 cm thick) explosions along the other sides of the solid Cu. The amatol was initiated from the bottom end of the system as shown above. The dotted and solid lines have the same meaning as described under Fig. 6.

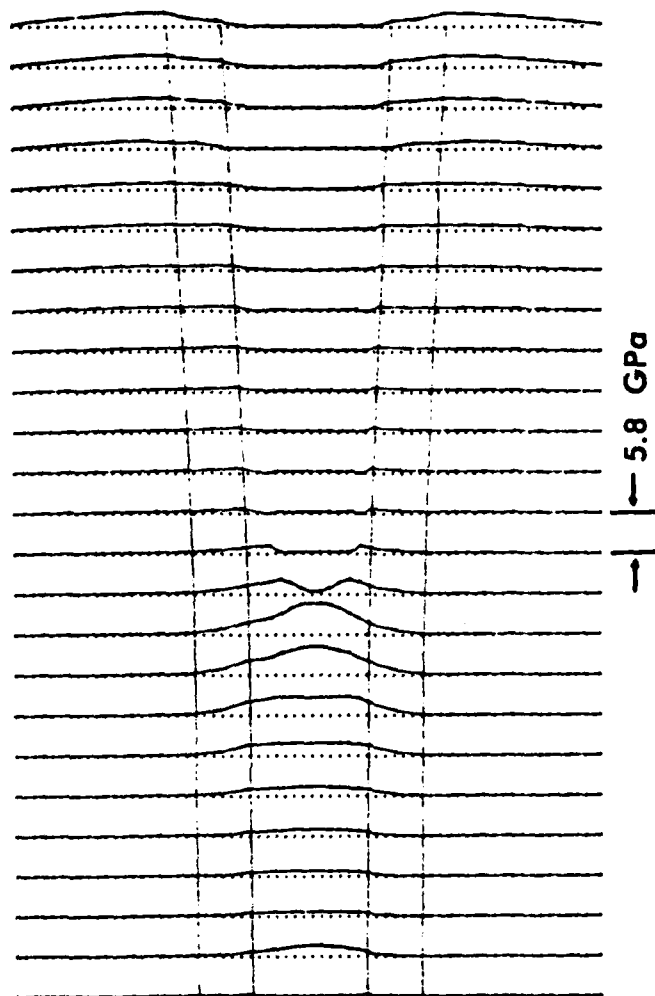


Figure 8. Computed compaction of porous Cu (60 percent of theoretical density). While only incomplete compaction was attained in the computation illustrated in Fig. 7, complete compaction is indicated above with the high pressures developed in the compressed powder. Even though only 2.0 cm of amatol was detonated on each side of the container - powder system in this case, total compaction was attained because the initial powder density was higher than for the computation illustrated in Fig. 7. The dotted and solid lines have the same meaning as described under Fig. 6.

REFERENCES

1. B. M. Dobratz, "LLNL Explosives Handbook. Properties of Chemical Explosives and Explosive Simulants," Lawrence Livermore National Laboratory Report No. UCRL-52997, March 1981.
2. L. Penn, F. Helm, M. Finger, and E. Lee, "Determination of Equation of State Parameters for Four Types of Explosives," Lawrence Livermore Laboratory Report No. UCRL-51892, August 1975.
3. B. Crossland and J. A. Cave, Proceedings, 5th International Conference on High Energy Rate Fabrication, University of Denver Research Institute, Colorado, 1975, pp 4.9.0-4.9.11.
4. M. A. Cook, E. B. Mayfield, and W. S. Partridge, "Reaction Rates of Ammonium Nitrate in Detonation," J. Phys. Chem., 59, 1955, pp 675-680.
5. H. C. Hoenig, E. L. Lee, M. Finger, and J. E. Kurrle, "Equation of State of Detonation Products," Proceedings, 5th Symposium (International) on Detonation, Ed. S. J. Jacobs and R. Roberts, Superintendent of Documents, Washington, D.C., 1970, pp 503-512.
6. J. Ribovich, R. W. Watson, and F. C. Gibson, "Instrumented Card-Gap Test," AIAA J., 6, 1968, pp 1260-1263.
7. L. Seaman and D. R. Curran, "TROT Computer Program for Two-Dimensional Stress Wave Propagation," Ballistic Research Laboratory Contract Report No. ARBRL-CR-00428, April 1980 (Unclassified) (AD A085766).
8. Lynn Seaman, Robert E. Tokheim, and Donald R. Curran, "Computational Representation of Constitutive Relations for Porous Materials," Defense Nuclear Agency Contract Report No. DNA 3412F, May 1974 (Unclassified).

DISTRIBUTION LIST

<u>No. of Copies</u>	<u>Organization</u>	<u>No. of Copies</u>	<u>Organization</u>
12	Commander Defense Technical Info Center ATTN: DTIC-DDA Cameron Station Alexandria, VA 22314	3	Commander US Army Armament Research and Development Command ATTN: DRDAR-TSS E. Bloore Dover, NJ 07801
3	Director Defense Advanced Research Projects Agency ATTN: Tech Info Dr. Edward C. Van Reuth Dr. Steve Fishman 1400 Wilson Boulevard Arlington, VA 22209	1	Director US Army ARRADCOM Benet Weapons Laboratory ATTN: DRDAR-LCB-TL Watervliet, NY 12189
1	Commander US Army Command and General Staff College ATTN: Archives Fort Leavenworth, KS 66027	1	Commander US Army Armament Materiel Readiness Command ATTN: DRSAR-LEP-L Rock Island, IL 61299
1	Deputy Assistant Secretary of the Army (R&D) Department of the Army Washington, DC 20310	1	Commander US Army Watervliet Arsenal Watervliet, NY 12189
1	Commander US Army War College ATTN: Lib Carlisle Barracks, PA 17013	1	Commander US Army Aviation Research and Development Command ATTN: DRSAR-E 4300 Goodfellow Blvd St. Louis, MO 63120
1	Commander US Military Academy ATTN: Library West Point, NY 10996	1	Director US Army Air Mobility Research and Development Laboratory Ames Research Center Moffett Field, CA 94035
1	Commander US Army Materiel Development and Readiness Command ATTN: DRCDMD-ST 5001 Eisenhower Avenue Alexandria, VA 22333	1	Commander US Army Communications Research and Development Command ATTN: DRSEL-ATDD Fort Monmouth, NJ 07703
1	Commander US Army Armament Research and Development Command ATTN: DRDAR-TDC (Dr. D. Gyorog) Dover, NJ 07801	1	Commander US Army Electronics Research and Development Command Technical Support Activity ATTN: DELSD-L Fort Monmouth, NJ 07703

DISTRIBUTION LIST

<u>No. of Copies</u>	<u>Organization</u>	<u>No. of Copies</u>	<u>Organization</u>
1	Commander US Army Harry Diamond Laboratory ATTN: DELHD-TA-L 2800 Powder Mill Road Adelphi, MD 20783	1	Director US Army TRADOC Systems Analysis Activity ATTN: ATAA-SL White Sands Missile Range NM 88002
1	Commander US Army Missile Command ATTN: DRSMI-R Redstone Arsenal, AL 35898	1	Office of Naval Research ATTN: Code 402 Dept of the Navy, 800 N. Quincy St Arlington, VA 22217
2	Commander US Army Missile Command ATTN: DRSMI-YDL Dr. Raymond Conrad Redstone Arsenal, AL 35898	1	Commander Naval Research Laboratory ATTN: Code 2020, Tech Lib Washington, DC 20375
2	Commander US Army Mobility Equipment Research & Development Cmd ATTN: DRDME-WC DRSME-RZT Fort Belvoir, VA 22060	1	AFWL/SUL Kirtland AFB, NM 87117
1	Commander US Army Tank Automotive Command ATTN: DRDTA-TSL Warren, MI 48090	1	Air Force Wright Aeronautical Laboratories Air Force Systems Command Materials Laboratory Wright-Patterson AFB, OH 45433
1	Commander US Army Materials and Mechanics Research Center ATTN: DRXMR-ATL Watertown, MA 02172	2	The Johns Hopkins University ATTN: Prof. R. B. Pond, Sr. Prof. R. Green 34th and Charles Streets Baltimore, MD 21218
1	Commander US Army Research Office P. O. Box 12211 Research Triangle Park NC 27709	2	Commandant US Army Infantry School ATTN: ATSH-CD-CSO-OR Fort Benning, GA 31905
2	Commander US Army Research and Standardization Group (Europe) ATTN: Dr. B. Steverding Dr. F. Rothwarf Box 65 FPO NY 09510		

DISTRIBUTION LIST

No. of
Copies

Organization

Aberdeen Proving Ground

Dir, USAMSAA
ATTN: DRXSY-D
DRXSY-MP, H. Cohen

Cdr, USATECOM
ATTN: DRSTE-TO-F

Dir, USACSL, EA
ATTN: DRDAR-CLB-PA
DRDAR-CLN
DRDAR-CLJ-L

USER EVALUATION OF REPORT

Please take a few minutes to answer the questions below; tear out this sheet, fold as indicated, staple or tape closed, and place in the mail. Your comments will provide us with information for improving future reports.

1. BRL Report Number _____

2. Does this report satisfy a need? (Comment on purpose, related project, or other area of interest for which report will be used.)

3. How, specifically, is the report being used? (Information source, design data or procedure, management procedure, source of ideas, etc.) _____

4. Has the information in this report led to any quantitative savings as far as man-hours/contract dollars saved, operating costs avoided, efficiencies achieved, etc.? If so, please elaborate.

5. General Comments (Indicate what you think should be changed to make this report and future reports of this type more responsive to your needs, more usable, improve readability, etc.) _____

6. If you would like to be contacted by the personnel who prepared this report to raise specific questions or discuss the topic, please fill in the following information.

Name: _____

Telephone Number: _____

Organization Address: _____

----- FOLD HERE -----

Director
US Army Ballistic Research Laboratory
ATTN: DRSMC-BLA-S (A)
Aberdeen Proving Ground, MD 21005



NO POSTAGE
NECESSARY
IF MAILED
IN THE
UNITED STATES

OFFICIAL BUSINESS
PENALTY FOR PRIVATE USE, \$300

BUSINESS REPLY MAIL
FIRST CLASS PERMIT NO 12062 WASHINGTON, DC
POSTAGE WILL BE PAID BY DEPARTMENT OF THE ARMY

Director
US Army Ballistic Research Laboratory
ATTN: DRSMC-BLA-S (A)
Aberdeen Proving Ground, MD 21005



----- FOLD HERE -----

DATE
ILME